Perturbative study of the Kitaev model with spontaneous time-reversal symmetry breaking

Sébastien Dusuel,[1,*] Kai Phillip Schmidt,[2,†] Julien Vidal,[3,‡] and Rosa Letizia Zaffino[3,§]

[1]*Lycée Louis Thuillier, 70 Boulevard de Saint Quentin, 80098 Amiens Cedex 3, France*

[2]*Lehrstuhl für theoretische Physik, Otto-Hahn-Straße 4, D-44221 Dortmund, Germany*

[3]*Laboratoire de Physique Théorique de la Matière Condensée, CNRS UMR 7600, Université Pierre et Marie Curie,*
4 Place Jussieu, 75252 Paris Cedex 05, France

We analyze the Kitaev model on the triangle-honeycomb lattice whose ground state has recently been shown to be a chiral spin liquid. We consider two perturbative expansions: the isolated-dimer limit containing Abelian anyons and the isolated-triangle limit. In the former case, we derive the low-energy effective theory and discuss the role played by multiplaquette interactions. In this phase, we also compute the spin-spin correlation functions for any vortex configuration. In the isolated-triangle limit, we show that the effective theory is, at lowest nontrivial order, the Kitaev honeycomb model at the isotropic point. We also compute the next-order correction which opens a gap and yields non-Abelian anyons.

I. INTRODUCTION

In two dimensions, particles may obey nontrivial braiding statistics.[1,2] However, a direct observation of these so-called anyons remains one of the most challenging topics in physics. Several good candidates have emerged in the last years among which was the fractional quantum Hall effect[3] but the braiding of Laughlin quasiparticles has still not been performed despite recent proposals based on Mach-Zehnder interferometer.[4]

Interestingly, at a theoretical level, such exotic excitations may also arise in spin systems.[5,6] A simple example is provided by the so-called toric code whose elementary excitations are known to behave as semions.[6] Nevertheless, this model is difficult to implement because it is based on four-spin interactions which are not easily reproduced in experimental setups. A better candidate is undoubtedly the Kitaev honeycomb model[7] which involves only two-spin interactions. Indeed, such a system may be realized experimentally in optical lattices either with cold atoms[8–10] or with polar molecules.[11] Furthermore, in a suitable parameter range, a perturbative low-energy effective model of the honeycomb model is the toric code[6] extended with multianyon interactions.[12] One must however keep in mind that, in the honeycomb model, one also has fermionic excitations which have to be taken into account when braiding anyons.[13] The honeycomb model has attracted much attention recently[12,14–16] because it can additionally be solved exactly via different fermionization methods (Majorana fermions[7] or Jordan-Wigner transformations[17]).

One of the most interesting extensions of this model suggested in Kitaev's seminal paper[7] has been proposed by Yao and Kivelson[18] who considered the same kind of model but on the triangle-honeycomb lattice. Indeed, in the presence of closed paths with an odd number of sites, the system spontaneously breaks the time-reversal symmetry and has two topologically distinct gapped phases characterized by Abelian and non-Abelian excitations. In their study, Yao and Kivelson[18] showed that the ground state is a chiral spin liquid associated to an odd Chern number (note that such an exotic state of matter has also been found in another spin model[19]). Their whole analysis relies on an exact treatment of the vortex-free sector (see below for details) which allows them to compute the fermionic gap. However, as in the honeycomb model, although the ground state belongs to this subspace, the low-energy states are known to lie in other vortex sectors for a wide range of parameters in the Abelian phase. In contrast, near the transition point, the fermionic gap in the vortex-free sector is smaller than the vortex gap.[18] The aim of this paper is to analyze this low-energy spectrum following and extending the procedure developed in Ref. 12 for the honeycomb model.

This paper is organized as follows. In Sec. II, we introduce the Kitaev model on the triangle-honeycomb lattice and discuss its symmetries. Section III is devoted to the perturbative treatment in the isolated-dimer limit. There, we first map the spin model onto an effective spin-boson system which is well suited to our analysis. We show that the low-energy effective Hamiltonian is related to the toric code on the honeycomb lattice although, at lowest nontrivial order (six), one only has magneticlike operators. This straightforwardly implies that the low-energy excitations are Abelian anyons with a semionic mutual statistics. We also compute the two-spin correlation functions for any vortex configuration up to order 6 and check our results for two simple vortex configurations (vortex free and vortex full) which allow for nonperturbative calculations. Finally, in Sec. IV, we consider the isolated-triangle limit; we show that the effective low-energy Hamiltonian is, at lowest order (one), exactly the Kitaev honeycomb model at the isotropic point. The next-order correction involves three-spin interactions as well as triangular-plaquette degrees of freedom. In the vortex-free sector, this term is exactly the one studied by Kitaev,[7] which opens a gap and gives rise to non-Abelian excitations. Contrary to the isolated-dimer limit, one cannot diagonalize the effective Hamiltonian for arbitrary vortex configurations. Thus, we focus on the vortex-free sector and compute the fermionic gap in this limit, which is a check of our perturbative expansion.
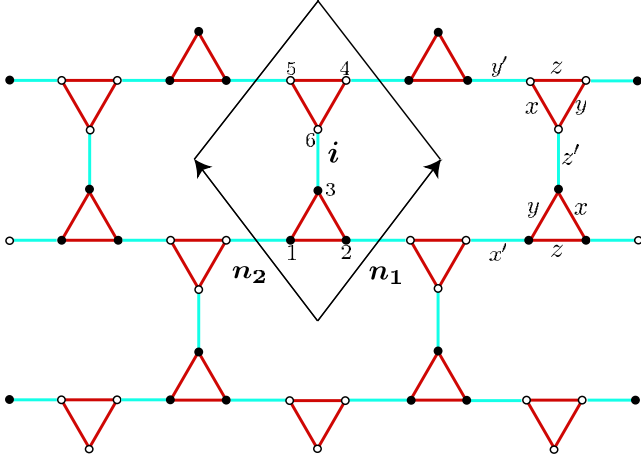
FIG. 1. (Color online) A piece of the triangle-honeycomb lattice which has six sites per unit cell.

II. MODEL

We consider the Kitaev model on the triangle-honeycomb lattice obtained by replacing each site of the honeycomb lattice by a triangle and described by the following Hamiltonian:

$$H = -\sum_\alpha \left[\sum_{\alpha \text{ links}} J_\alpha \sigma_i^\alpha \sigma_j^\alpha + \sum_{\alpha' \text{ links}} J'_\alpha \sigma_i^\alpha \sigma_j^\alpha \right], \quad (1)$$

where α takes values x, y, or z, and links of type x, y, z or x', y', z' are illustrated in Fig. 1. In the above formula, i and j are the two sites of the α or α' link and the σ_i^α's are the usual Pauli matrices at site i. Without loss of generality,[7] we also consider ferromagnetic interactions $J_\alpha, J'_\alpha > 0$. This lattice contains six sites per unit cell and two kinds of elementary plaquettes: triangles and dodecagons. As in the original Kitaev honeycomb model, H commutes with all plaquette operators defined as $W_p = \Pi_{i \in p} \sigma_i^{\text{out}(i)}$, where out$(i)$ denotes the outgoing direction at site i with respect to the plaquette p. Note that with this definition, plaquette operators have real eigenvalues $w_p = \pm 1$, whereas, with the convention proposed in Ref. 7, one has $w_p = \pm i$ for odd-loop operators.

As suggested in Ref. 18, in the following, we further set

$$J_x = J_y = J_z = J, \quad J'_x = J'_y = J'_z = J', \quad (2)$$

so that the Hamiltonian H respects the symmetries of the lattice. It is also time-reversal invariant since it is quadratic in the spin operators. However, as explained by Kitaev,[7] the presence of closed paths with an odd number of sites (here due to triangles) breaks this symmetry spontaneously. This symmetry breaking may be understood by noting that changing the flux of all triangles, i.e., flipping their W_p's, does not change the energy so that each eigenstate is, at least, twofold degenerate.[18]

As in the Kitaev honeycomb model,[6] the Hamiltonian H can be mapped onto a free (Majorana) fermion problem which allows for an exact solution. Thus, in each vortex sector defined by a configuration of the W_p's one has a fermionic spectrum. Nevertheless, the low-energy states may be given by ground states of other vortex sectors and, when the

corresponding flux configurations are not translation invariant, one is led to solve an impuritylike problem. In Ref. 18, Yao and Kivelson numerically showed that the ground state of H always lies in the vortex-free sector ($w_p = +1$ for all p) and supported this analysis by perturbative considerations.[20] In the following, we shall see that this is verified in the first perturbative limit we consider (isolated dimers), whereas we did not manage to prove it in the other limit. In addition, in the isolated-dimer limit described in Sec. III, we compute the low-energy spectrum for all vortex configurations and give a perturbative expansion of the anyonic gap.

III. ISOLATED-DIMER LIMIT

A. Mapping onto an effective spin-boson problem

Our goal is to perform a perturbative analysis of the Abelian phase around the isolated-dimer limit $J' \gg J$. To do so, we shall use the effective spin-boson mapping introduced in Ref. 12 but, for convenience, let us first perform the following rotations:

$$\sigma_{1,i}^\alpha \Rightarrow \tilde{\sigma}_{1,i}^{\mathcal{C}^2(\alpha)}, \quad \sigma_{2,i}^\alpha \Rightarrow \tilde{\sigma}_{2,i}^{\mathcal{C}(\alpha)}, \quad \sigma_{3,i}^\alpha \Rightarrow \tilde{\sigma}_{3,i}^\alpha, \quad (3)$$

$$\sigma_{4,i}^\alpha \Rightarrow \tilde{\sigma}_{4,i}^{\mathcal{C}^2(\alpha)}, \quad \sigma_{5,i}^\alpha \Rightarrow \tilde{\sigma}_{5,i}^{\mathcal{C}(\alpha)}, \quad \sigma_{6,i}^\alpha \Rightarrow \tilde{\sigma}_{6,i}^\alpha, \quad (4)$$

where $\mathcal{C}$ is the cycle operator which maps (x,y,z) onto (y,z,x). Here, each site is encoded by a cell index $\boldsymbol{i}$ and a position index $k = 1, \ldots, 6$ inside the cell as shown in Fig. 1. Hamiltonian (1) then reads

$$H = -J \sum_i \tilde{\sigma}_{1,i}^y \tilde{\sigma}_{2,i}^x + \tilde{\sigma}_{2,i}^y \tilde{\sigma}_{3,i}^x + \tilde{\sigma}_{3,i}^y \tilde{\sigma}_{1,i}^x$$

$$- J \sum_i \tilde{\sigma}_{4,i}^y \tilde{\sigma}_{5,i}^x + \tilde{\sigma}_{5,i}^y \tilde{\sigma}_{6,i}^x + \tilde{\sigma}_{6,i}^y \tilde{\sigma}_{4,i}^x$$

$$- J' \sum_i \tilde{\sigma}_{1,i}^z \tilde{\sigma}_{4,i-n_1}^z + \tilde{\sigma}_{2,i}^z \tilde{\sigma}_{5,i-n_2}^z + \tilde{\sigma}_{3,i}^z \tilde{\sigma}_{6,i}^z. \quad (5)$$

With this transformation, the interaction term on each dimer (i,j) displayed in cyan in Fig. 1 is simply $\tilde{\sigma}_i^z \tilde{\sigma}_j^z$. Denoting $|\uparrow\rangle$ $(|\downarrow\rangle)$ as the eigenstate of $\tilde{\sigma}^z$ with eigenvalue of $+1$ (-1), each cyan dimer can be in four different states,

$$\{|\uparrow\uparrow\rangle, |\downarrow\downarrow\rangle\} \quad \text{with energy} \quad -J',$$

$$\{|\uparrow\downarrow\rangle, |\downarrow\uparrow\rangle\} \quad \text{with energy} \quad +J'. \quad (6)$$

An alternative description of these four states consists in interpreting the low-energy (ferromagnetic) states as two effective spin states without a quasiparticle and the high-energy (antiferromagnetic) states as two effective spin states with one quasiparticle. The energy gap between these states is $\Delta = 2J'$ and corresponds to the fermionic gap evoked in Sec. II. In the following, we set once for all $J' = 1/2$ or equivalently $\Delta = 1$. Among the possible mappings we choose the following:[12]

$$|\uparrow\uparrow\rangle = |\Uparrow 0\rangle, \quad |\downarrow\downarrow\rangle = |\Downarrow 0\rangle, \quad |\uparrow\downarrow\rangle = |\Uparrow 1\rangle, \quad |\downarrow\uparrow\rangle = |\Downarrow 1\rangle,$$
$$(7)$$

where the left (right) spin is the one of the black (white) site of the dimer and double arrows represent the state of the effective spin.

Within this framework, each dimer is reduced to a single site with 4 degrees of freedom [one effective spin 1/2 and a hardcore boson occupation number (0 or 1)]. Considering that each site (• or ∘, see Fig. 1) of the triangle-honeycomb lattice belongs to a cyan dimer, one then has

$$\tilde{\sigma}^x_{i,\bullet} = \tau^x_i(b^\dagger_i + b_i), \quad \tilde{\sigma}^x_{i,\circ} = b^\dagger_i + b_i,$$

$$\tilde{\sigma}^y_{i,\bullet} = \tau^y_i(b^\dagger_i + b_i), \quad \tilde{\sigma}^y_{i,\circ} = i\tau^z_i(b^\dagger_i - b_i),$$

$$\tilde{\sigma}^z_{i,\bullet} = \tau^z_i, \quad \tilde{\sigma}^z_{i,\circ} = \tau^z_i(1 - 2b^\dagger_i b_i), \quad (8)$$

where τ^α_i's are Pauli matrices acting on the effective spin and $b^\dagger_i$ (b_i) is the creation (annihilation) operator of a hardcore boson at site i which obeys

$$[b_i, b^\dagger_j] = \delta_{ij}(1 - 2b^\dagger_i b_i). \quad (9)$$

Hamiltonian (5) then reads

$$H = -\frac{N}{2} + Q + T_0 + T_{+2} + T_{-2}, \quad (10)$$

where N is the number of cyan dimers, $Q = \Sigma_i b^\dagger_i b_i$,

$$T_0 = -J \sum_i (t^{2,i}_{1,i} + t^{3,i}_{2,i} + t^{1,i}_{3,i} + t^{2,i+n_2}_{1,i+n_1} + t^{3,i}_{2,i+n_2} + t^{1,i+n_1}_{3,i}) + \text{H.c.}, \quad (11)$$

$$T_{+2} = T^\dagger_{-2} = -J \sum_i (v^{2,i}_{1,i} + v^{3,i}_{2,i} + v^{1,i}_{3,i} + v^{2,i+n_2}_{1,i+n_1} + v^{3,i}_{2,i+n_2} + v^{1,i+n_1}_{3,i}), \quad (12)$$

with hopping operators,

$$t^{2,i}_{1,i} = b^\dagger_{2,i} b_{1,i} \tau^y_{1,i} \tau^x_{2,i}, \quad (13)$$

$$t^{3,i}_{2,i} = b^\dagger_{3,i} b_{2,i} \tau^y_{2,i} \tau^x_{3,i}, \quad (14)$$

$$t^{1,i}_{3,i} = b^\dagger_{1,i} b_{3,i} \tau^y_{3,i} \tau^x_{1,i}, \quad (15)$$

$$t^{2,i+n_2}_{1,i+n_1} = -i b^\dagger_{2,i+n_2} b_{1,i+n_1} \tau^z_{1,i+n_1}, \quad (16)$$

$$t^{3,i}_{2,i+n_2} = -i b^\dagger_{3,i} b_{2,i+n_2} \tau^z_{2,i+n_2}, \quad (17)$$

$$t^{1,i+n_1}_{3,i} = -i b^\dagger_{1,i+n_1} b_{3,i} \tau^z_{3,i}, \quad (18)$$

and pair-creation operators,

$$v^{2,i}_{1,i} = b^\dagger_{2,i} b^\dagger_{1,i} \tau^y_{1,i} \tau^x_{2,i}, \quad (19)$$

$$v^{3,i}_{2,i} = b^\dagger_{3,i} b^\dagger_{2,i} \tau^y_{2,i} \tau^x_{3,i}, \quad (20)$$

$$v^{1,i}_{3,i} = b^\dagger_{1,i} b^\dagger_{3,i} \tau^y_{3,i} \tau^x_{1,i}, \quad (21)$$
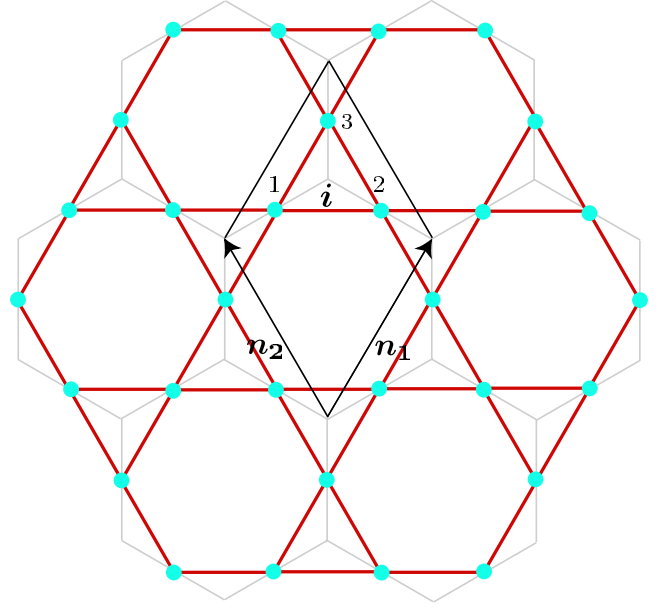

FIG. 2. (Color online) Effective kagome lattice obtained from the triangle-honeycomb lattice by replacing each dimer linking triangles by a site. We displayed in gray the "dual" honeycomb lattice on which the toric code is defined (see text).

$$v^{2,i+n_2}_{1,i+n_1} = i b^\dagger_{2,i+n_2} b^\dagger_{1,i+n_1} \tau^z_{1,i+n_1}, \quad (22)$$

$$v^{3,i}_{2,i+n_2} = i b^\dagger_{3,i} b^\dagger_{2,i+n_2} \tau^z_{2,i+n_2}, \quad (23)$$

$$v^{1,i+n_1}_{3,i} = i b^\dagger_{1,i+n_1} b^\dagger_{3,i} \tau^z_{3,i}. \quad (24)$$

Now, each site is encoded by a cell index i and its position inside the cell which takes three values $k = 1, 2, 3$ as shown in Fig. 2. Within this formalism, the plaquette operators read

$$W_\triangle = \prod_{i\in\triangle} \tau^z_i, \quad W_\triangledown = (-1)^{\Sigma_{i\in\triangledown} b^\dagger_i b_i} \prod_{i\in\triangledown} \tau^z_i \quad (25)$$

for triangles and

$$W_\bigcirc = (-1)^{b^\dagger_{2,i} b_{2,i+n_2} + b^\dagger_{1,i-n_2} b_{1,i-n_2} + b^\dagger_{3,i-n_1} b_{3,i-n_1}} \prod_{i\in\bigcirc} \tau^y_i \quad (26)$$

for the dodecagonal plaquette (which are hexagonal in the effective lattice) located below the cell i (see notations in Fig. 2).

The main interest of this mapping is that the form of Hamiltonian (10) is especially adapted to the perturbative treatment developed in Sec. III B. Indeed, a key ingredient of our approach which is based on the continuous unitary transformations[21] together with the particle-number conserving generator[22–24] is that the energy spectrum of the unperturbed Hamiltonian has to be equidistant.

B. Perturbative analysis of the low-energy sector

In this section, we used exactly the same method as those described in Refs. 12 and 25 for the Kitaev honeycomb model. Therefore, we skipped all technical details and only give here the results of our calculations.

First, let us note that, in the triangle-honeycomb lattice, one has

$$N_s = 3N_t = 6N_d = 2N, \qquad (27)$$

where N is the number of cyan dimers and s, t, and d stand, respectively, for sites, triangles (so $N_t = N_\triangle + N_\triangledown$), and dodecagons (or effective hexagons, so $N_d = N_\bigcirc$). There are thus as many conserved $\mathbb{Z}_2$ plaquette operators $N_t + N_d$ as the number N of effective spin 1/2. This implies that in the low-energy subspace with no hardcore boson, the effective Hamiltonian can, in the isolated-dimer limit $J' \gg J$, be written only in terms of the plaquette operators and is thus readily solved. The general form of this effective Hamiltonian reads

$$H_{\text{eff}}^{(0)} = E_0 - \sum_{p_1, \dots, p_n} C_{p_1, \dots, p_n} W_{p_1} W_{p_2} \cdots W_{p_n}, \qquad (28)$$

where $p_1, \dots, p_n$ denotes a set of n plaquettes.

We performed this perturbative expansion of the effective Hamiltonian up to order 8 which is the lowest order involving multiplaquette interactions. At this order, the constant term is given by

$$\frac{E_0}{N} = -\frac{1}{2} - J^2 - \frac{1}{4}J^4 - \frac{1}{8}J^6 + \frac{15}{64}J^8. \qquad (29)$$

The first nontrivial contribution arises at order 6 where only hexagonal-plaquette operators are involved. At order 8, this latter term is renormalized and triangular-plaquette operators come into play. More precisely, one has

$$H_{\text{eff}}^{(0)} = E_0 - C_h \sum_h W_h - C_{h,t_1,t_2} \sum_{h,t_1,t_2} W_h W_{t_1} W_{t_2}, \qquad (30)$$

where the first sum is performed over all hexagonal plaquettes h (i.e., $\bigcirc$) and the second one over triplet plaquettes made of one hexagon h and two triangles t_1 and t_2 (of any kind $\triangle$ or $\triangledown$) adjacent to this hexagon. At order 8, the coefficients are given by

$$C_h = \frac{63}{8}J^6 - \frac{297}{8}J^8, \qquad C_{h,t_1,t_2} = \frac{33}{16}J^8. \qquad (31)$$

Thus, at order 6, the spectrum does not depend on the fluxes inside the triangles and this degeneracy is only partially lifted at order 8. Note that the signs of C_h and C_{h,t_1,t_2} confirm, in this limit, that (one of) the ground state lies in the vortex-free sector ($w_p = +1$ for all plaquettes) as conjectured in Ref. 18. In addition, we emphasize that triangular-plaquette operators appear by pairs which are reminiscent from the time-reversal symmetry that the effective Hamiltonian must satisfy (see Sec. II).

It is interesting to interpret this result in terms of plaquettes and vertex operators. Therefore, one may view the effective kagome lattice as a honeycomb lattice where each site lies in the middle of the triangles as shown in Fig. 2. Within this picture, the plaquette operators $W_\bigcirc$ are interpreted as flux (magnetic) operators, whereas $W_{\triangle,\triangledown}$ appear as vertex (electric) operators. In this gauge theory language used in the toric-code model,[6] our results show that, at lowest order, there is no contribution of the vertex operators.

Thus, the triangle-honeycomb lattice in this isolated-dimer limit does not map onto a standard toric-code-like problem. However, the eigenstates of the effective Hamiltonian are those of the toric code on the hexagonal lattice and, as such, display anyonic statistics. To be more precise, one must distinguish between electric and magnetic excitations which are localized on triangles and hexagons (in the kagome lattice), respectively. These two kinds of excitations have mutual semionic statistics[6,18] but they individually behave as bosons. Finally, let us remark that the gaps of magnetic excitations (order of magnitude J^6) and of electric excitations (order of magnitude J^8) are even smaller than the gap in the Kitaev honeycomb model (order of magnitude J^4). This would make an experimental detection of anyons in the triangle-honeycomb model even more problematic than in the honeycomb model.[13]

C. Correlation functions in the low-energy sector

As in the Kitaev honeycomb model, any correlator involving an odd number of spin operators vanishes although the eigenstates break the time-reversal symmetry. Indeed, as discussed by Yao and Kivelson,[18] every eigenstate is, at least, twofold degenerate since one can flip every triangular plaquette without changing the energy but *this operation is global*. Consequently, as in the honeycomb model,[15,26] the only nonvanishing correlators are products of $\sigma_i^\alpha \sigma_j^\alpha$ on an α dimers. Here, we focus on the simplest case involving only one such object, i.e., $C_{i,j}^{\alpha\alpha} = \langle \sigma_i^\alpha \sigma_j^\alpha \rangle$.

In the triangle-honeycomb model, one has, *a priori*, nine different functions to consider since the unit cell contains nine different dimers. However, with the choice of the couplings we made, one only has two different functions to distinguish: those on "weak" bonds (x, y, z links with interaction J) and those on "strong" bonds (x', y', z' links with interaction J'). As for the low-energy spectrum, one expects a plaquette-operator expansion as in Eq. (28). We performed the calculation of these two correlation functions up to order 6 and obtained

$$C_{i,j}^{\text{strong}} = 1 - 2J^2 - \frac{3}{2}J^4 - \frac{5}{4}J^6 - \frac{105}{8}J^6(W_{p_1} + W_{p_2}), \quad (32)$$

where p_1 and p_2 are the two dodecagonal plaquettes shared by the considered strong bond (i,j). Similarly, since we set $J_x = J_y$, we found for a weak bond (i,j)

$$C_{i,j}^{\text{weak}} = J + \frac{1}{2}J^3 + \frac{3}{8}J^5 + \frac{63}{8}J^5 W_p, \qquad (33)$$

where p is the dodecagonal plaquette adjacent to the considered bond.

As can be seen from Eqs. (32) and (33), the presence of a vortex is detected at orders 6 and 5, respectively. This difference stems from the fact that one analyzes the isolated-dimer limit for which, at lowest order, $C_{i,j}^{\text{strong}} = 1$ whereas $C_{i,j}^{\text{weak}} = 0$.

D. Checks from Majorana fermions

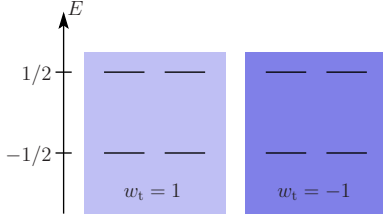To check our results we computed exactly the ground-state energy in the vortex-free (full) sector for which $w_p =$

FIG. 3. (Color online) Spectrum of an isolated triangle with $J = \frac{1}{2\sqrt{3}}$. The eigenstates have quantum number $w_t = 1$ (left) or $w_t = -1$ (right).

+1 (−1) for all p using Majorana fermions as described by Kitaev for the honeycomb model.[7] Following, the procedure described in Ref. 25, we performed a perturbative expansion of the exact solutions order by order. Denoting e_0^ν the ground-state energy per cyan dimer for a vortex filling factor $\nu = \frac{\text{No. of vortex}}{\text{No. of plaquette}}$ one gets

$$e_0^{\nu=0} = -J' - \frac{J^2}{2J'} - \frac{J^4}{32J'^3} - \frac{11J^6}{128J'^5} + \frac{147J^8}{8192J'^7}, \quad (34)$$

$$e_0^{\nu=1} = -J' - \frac{J^2}{2J'} - \frac{J^4}{32J'^3} + \frac{5J^6}{64J'^5} - \frac{117J^8}{8192J'^7}. \quad (35)$$

Keeping in mind that the number of hexagons is $N/3$ and that for each hexagon h there are 15 triplets h, t_1, t_2, these results are straightforwardly recovered using Eqs. (29)–(31).

One can also check the expression of the correlation functions in these vortex configurations. Indeed, the Hellmann-Feynman theorem states that

$$\frac{\partial e_0^\nu}{\partial J'} = -\frac{1}{N} \sum_{(i,j)} C_{i,j}^{\text{strong}} = -C_{i,j}^{\text{strong}}, \quad (36)$$

$$\frac{\partial e_0^\nu}{\partial J} = -\frac{1}{N} \sum_{(i,j)} C_{i,j}^{\text{weak}} = -2 C_{i,j}^{\text{weak}}, \quad (37)$$

where the sum in Eq. (36) [Eq. (37)] is performed over all strong bonds (weak bonds) in the initial lattice. The last equalities stem from the fact that for $\nu = 0, 1$ every plaquette has the same contribution which would not be true for other vortex configurations. Using Eqs. (34) and (35) and the above relations, one can easily check the validity of Eqs. (32) and (33).

IV. ISOLATED-TRIANGLE LIMIT

A. Mapping to a spin-boson plaquette problem

Let us now turn to the isolated-triangle limit $J \gg J'$. These triangles live on the sites of an effective hexagonal lattice. For convenience, we use rotated form (5) that was already used in the isolated-dimer limit. The spectrum of the Hamiltonian of an isolated triangle is made of two sets of fourfold-degenerate levels. In each of these sets, two levels have eigenvalue $w_t = 1$ and the other two $w_t = -1$. Setting $J = \frac{1}{2\sqrt{3}}$, the eigenenergies are $\pm 1/2$. This information is gathered in Fig. 3.
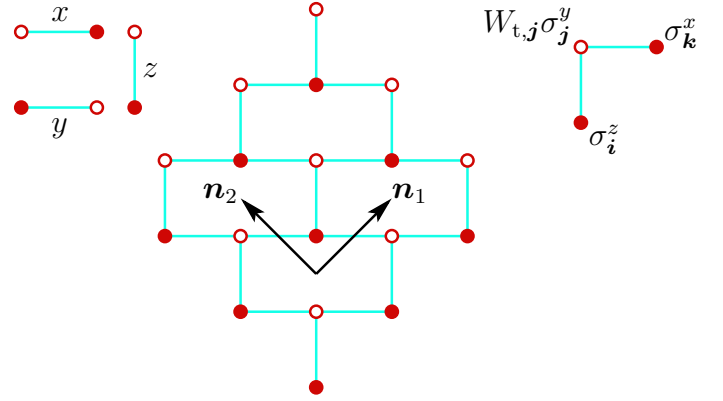

FIG. 4. (Color online) A piece of the effective brickwall lattice spanned by triangles, together with the notations for x, y, and z links (left). Filled (empty) dots represent the triangles made of filled (empty) dots in Fig. 1. On the right, we have represented one of the second-order three-spin terms that appear in Eq. (48).

As in the isolated-dimer limit, we interpret low (high) energy states of an isolated triangle as containing zero (one) hardcore boson. This hardcore boson degree of freedom, which we again denote as b, together with the $\mathbb{Z}_2$ quantum number w_t span a four-dimensional Hilbert space. It is then natural to introduce an effective spin 1/2 to span the full eight-dimensional Hilbert space of a triangle. We again denote this effective spin as τ (though it is not the same as in the other perturbative limit, and the same remark holds for b). The way this effective spin is introduced is partly dictated by the operators involved in the adjacent dodecagonal-plaquette operators. For the triangle 1,2,3 of Fig. 1 (and dropping the i index), the mapping reads

$$\tau^x = W_t \tilde{\sigma}_2^x \tilde{\sigma}_3^y, \quad \tau^y = W_t \tilde{\sigma}_3^x \tilde{\sigma}_1^y, \quad \tau^z = -W_t \tilde{\sigma}_1^x \tilde{\sigma}_2^y. \quad (38)$$

It is straightforward to check that the above τ^α operators satisfy the usual Pauli matrix algebra. The product $\tilde{\sigma}_2^x \tilde{\sigma}_3^y$ appearing in τ^x, for example, is the same as the one that appears in the dodecagonal-plaquette operator having bond 2,3 in common with the triangle. It is interesting to note that one has to use the operator $W_t = \tilde{\sigma}_1^z \tilde{\sigma}_2^z \tilde{\sigma}_3^z$ to fulfill the SU(2) algebra. The same mapping is used for the other triangles, with 1,2,3 simply replaced by 4,5,6 (see Fig. 1 for notations).

Since the terms proportional to J in Eq. (5) now read $-N_t/2 + Q$, with $Q = \Sigma_i b_i^\dagger b_i$ where the sum runs over the sites i of the effective hexagonal lattice (formed by triangles), the last task in rewriting Hamiltonian (5) is to find the new form of the terms proportional to J'. A simple but lengthy calculation yields

$$H = -N_t/2 + Q - \frac{J'}{3} \sum_{\alpha=x,y,z} \sum_{\alpha \text{ links}} \mathcal{O}_i^\alpha \mathcal{O}_j^\alpha, \quad (39)$$

where α indicates a link of type x, y, or z on the honeycomb or equivalently brickwall lattice, with the conventions of Kitaev,[7] as shown in Fig. 4. Furthermore i and j are the sites

of the effective brickwall lattice on link α, and the operators $\mathcal{O}_i^\alpha$ read ($W_{\mathrm{t},i}$ denotes the triangular-plaquette operator which is now associated to site i)

$$\mathcal{O}_i^\alpha = \tau_i^\alpha \{ (-1)^{b_i^\dagger b_i} - \sqrt{2} W_{\mathrm{t},i} [e^{(2i\pi/3) p^\alpha W_{\mathrm{t},i}} b_i^\dagger + \mathrm{H.c.}] \}, \quad (40)$$

where $p^x = 1$, $p^y = -1$, and $p^z = 0$.

B. Perturbation analysis of the low-energy sector

From the above expressions, it is clear that the Hamiltonian can now be written

$$H = -\frac{N_{\mathrm{t}}}{2} + Q + T_0 + T_{+1} + T_{-1} + T_{+2} + T_{-2}, \quad (41)$$

where the operators T_n change the number of bosons by n and are proportional to J'. With our notations, they read

$$T_n = -\frac{J'}{3} \sum_{\alpha=x,y,z} \sum_{\alpha \text{ links}} \tau_i^\alpha \tau_j^\alpha \mathcal{T}_{n,i,j}^\alpha, \quad (42)$$

with

$$\mathcal{T}_{0,i,j}^\alpha = (-1)^{b_i^\dagger b_i + b_j^\dagger b_j} + 2 W_{\mathrm{t},i} W_{\mathrm{t},j} [e^{(2i\pi/3) p^\alpha (W_{\mathrm{t},i} - W_{\mathrm{t},j})} b_i^\dagger b_j + \mathrm{H.c.}], \quad (43)$$

$$\mathcal{T}_{1,i,j}^\alpha = -\sqrt{2} [W_{\mathrm{t},i} e^{(2i\pi/3) p^\alpha W_{\mathrm{t},i}} b_i^\dagger (-1)^{b_j^\dagger b_j} + (i \leftrightarrow j)], \quad (44)$$

$$\mathcal{T}_{2,i,j}^\alpha = 2 W_{\mathrm{t},i} W_{\mathrm{t},j} e^{(2i\pi/3) p^\alpha (W_{\mathrm{t},i} + W_{\mathrm{t},j})} b_i^\dagger b_j^\dagger, \quad (45)$$

$$T_{-1} = T_1^\dagger, \quad T_{-2} = T_2^\dagger. \quad (46)$$

As in the isolated-dimer limit (where $T_{\pm 1}$ terms are absent), with a suitable unitary transformation, such a Hamiltonian can be recast in a unitary equivalent effective form H_{eff} which conserves the number of bosons, i.e., that commutes with Q. We refer the reader to Ref. 24 (especially Appendix B), from which it follows that at order 2,

$$H_{\mathrm{eff}} = -\frac{N_{\mathrm{t}}}{2} + Q + T_0 + [T_{+1}, T_{-1}] + \frac{1}{2} [T_{+2}, T_{-2}]. \quad (47)$$

A tedious calculation then shows that in the low-energy subspace with no boson, the effective Hamiltonian (still at order 2) has the form

$$H_{\mathrm{eff}}^{(0)} = -\frac{N_{\mathrm{t}}}{2} (1 + 2 J'^2) - \frac{J'}{3} \sum_\alpha \sum_{\alpha \text{ links}} \tau_i^\alpha \tau_j^\alpha$$
$$+ \frac{2\sqrt{3} J'^2}{9} \sum_{i,j,k} W_{\mathrm{t},j} \tau_i^\alpha \tau_j^\beta \tau_k^\gamma. \quad (48)$$

The low-energy effective Hamiltonian at order 1 is nothing but that of the Kitaev honeycomb model at the isotropic point, though one should remember that site i now also has the $\mathbb{Z}_2$ supplementary degree of freedom $W_{\mathrm{t},i}$. In Eq. (48), the

last (primed) sum is to be taken over all possible combinations of three sites i, j, and k such that i and k are nearest neighbors of j and the spin "directions" α, β, and γ are such that (i,j) is an α link, (j,k) is a γ link, and β is the outgoing direction at site j of the path (i,j,k) (note that α, β, and γ are all distinct). For clarity, one such term is illustrated in Fig. 4 (right). These terms, apart from the plaquette operator $W_{\mathrm{t},j}$, are exactly the ones that arise when switching a magnetic field on in the gapless phase of the Kitaev honeycomb model. They open a gap and give proper non-Abelian anyonic statistics to the vortices, as detailed in Ref. 7. Actually, one does not know how to diagonalize analytically $H_{\mathrm{eff}}^{(0)}$ for arbitrary vortex configurations even at order 1[7] and, in particular, how to obtain the ground state of each sector. Therefore, contrary to the isolated-dimer limit, one cannot compute the correlation functions in this limit.

Let us remark that the plaquette operators on an elementary brick (or hexagon) h—namely, $W_h = \Pi_{i \in h} \tau_i^{\mathrm{out}(i)}$—are the product of the plaquette operators of the corresponding dodecagon on the original lattice *and* of its adjacent triangles, as follows from Eq. (38). From Eq. (48) and the previous remarks, it follows that the vortex-free sector contains non-Abelian anyons, which is consistent with the findings of Ref. 18. One can also use Kitaev's result (see Sec. 8 of Ref. 7) to obtain the gap in this sector,

$$\Delta = 6\sqrt{3} \times \frac{2\sqrt{3} J'^2}{9} = 4 J'^2, \quad (49)$$

in units where $J = \frac{1}{2\sqrt{3}}$ and thus also $\Delta = \frac{2\sqrt{3} J'^2}{3J}$ if J is chosen freely. This value of the gap is consistent with the numerical results obtained by Yao and Kivelson,[18] and we also checked it using an expansion of the exact result from Majorana fermionization. We also checked that the ground-state energies in the vortex-free sector obtained, thanks to a Majorana fermionization of Hamiltonian (48) or directly of initial Hamiltonian (1), match at order 2.

Finally, let us mention that at order 1, the ground states of Eq. (48) are such that $W_h = 1$ for all h. There are many such states. The vortex-free state is such a state, but any configuration where the six triangles surrounding one dodecagon are flipped to $W_{\mathrm{t}} = -1$ is also such a state, since every dodecagon is then surrounded by an even number of flipped triangles. From form (48) at order 2, we do not know how to prove that the ground state is the vortex-free state (we do not even know if this is true or if one has to go to higher orders in perturbation to prove it). We leave this as an open question.

V. CONCLUSION

In this work, we have studied perturbatively the Kitaev model on the triangle-honeycomb model. This has allowed us to show that in the isolated-dimer limit, the model has low-energy Abelian anyonic excitations, whereas in the isolated-triangle limit, the anyons become non-Abelian. This picture is consistent with the values of the Chern number in each of these phases.[18] In the isolated-dimer limit, we have furthermore computed the low-energy spectrum as well as the spin-spin correlation functions, which both display a

plaquette expansion. We emphasize that such a computation is not an easy task within the Majorana or Jordan-Wigner formalism, which are only well suited to study analytically configurations of vortices which display translational invariance.

---

*sdusuel@gmail.com

†schmidt@fkt.physik.uni-dortmund.de

‡vidal@lptmc.jussieu.fr

§zaffino@lptmc.jussieu.fr

[1] J. M. Leinaas and J. Myrheim, Nuovo Cimento Soc. Ital. Fis., B **37**, 1 (1977).

[2] F. Wilczek, Phys. Rev. Lett. **48**, 1144 (1982).

[3] F. E. Camino, W. Zhou, and V. J. Goldman, Phys. Rev. Lett. **95**, 246802 (2005).

[4] D. E. Feldman, Y. Gefen, A. Kitaev, K. T. Law, and A. Stern, Phys. Rev. B **76**, 085333 (2007).

[5] X.-G. Wen, Phys. Rev. Lett. **90**, 016803 (2003).

[6] A. Y. Kitaev, Ann. Phys. (N.Y.) **303**, 2 (2003).

[7] A. Kitaev, Ann. Phys. (N.Y.) **321**, 2 (2006).

[8] L.-M. Duan, E. Demler, and M. D. Lukin, Phys. Rev. Lett. **91**, 090402 (2003).

[9] L. Jiang, G. K. Brennen, A. V. Gorshkov, K. Hammerer, M. Hafezi, E. Demler, M. D. Lukin, and P. Zoller, Nat. Phys. **4**, 482 (2008).

[10] M. Aguado, G. K. Brennen, F. Verstraete, and J. I. Cirac, arXiv:0802.3163 (unpublished).

[11] A. Micheli, G. K. Brennen, and P. Zoller, Nat. Phys. **2**, 341 (2006).

[12] K. P. Schmidt, S. Dusuel, and J. Vidal, Phys. Rev. Lett. **100**, 057208 (2008).

[13] S. Dusuel, K. P. Schmidt, and J. Vidal, Phys. Rev. Lett. **100**, 177204 (2008).

[14] V. Lahtinen, G. Kells, A. Carollo, T. Stitt, J. Vala, and J. K. Pachos, Ann. Phys. (N.Y.) **323**, 2286 (2008).

[15] H.-D. Chen and Z. Nussinov, J. Phys. A **41**, 075001 (2008).

[16] K. Sengupta, D. Sen, and S. Mondal, Phys. Rev. Lett. **100**, 077204 (2008).

[17] H.-D. Chen and J. Hu, Phys. Rev. B **76**, 193101 (2007).

[18] H. Yao and S. A. Kivelson, Phys. Rev. Lett. **99**, 247203 (2007).

[19] D. F. Schroeter, E. Kapit, R. Thomale, and M. Greiter, Phys. Rev. Lett. **99**, 097202 (2007).

[20] H. Yao and S. A. Kivelson (unpublished).

[21] F. Wegner, Ann. Phys. (Leipzig) **3**, 77 (1994).

[22] J. Stein, J. Stat. Phys. **88**, 487 (1997).

[23] A. Mielke, Eur. Phys. J. B **5**, 605 (1998).

[24] C. Knetter and G. S. Uhrig, Eur. Phys. J. B **13**, 209 (2000).

[25] J. Vidal, K. P. Schmidt, and S. Dusuel (unpublished).

[26] G. Baskaran, S. Mandal, and R. Shankar, Phys. Rev. Lett. **98**, 247201 (2007).